Sains Malaysiana 54(12)(2025): 2859-2872
http://doi.org/10.17576/jsm-2025-5412-05

Integrated Investigation on the Synthesis, Computational Analysis, Thermal Stability, and Performance of Eco-Friendly Chelating Agents for Calcium Ions

(Penyelidikan Bersepadu tentang Sintesis, Analisis Pengkomputeran, Kestabilan Terma dan Prestasi Agen Pengkelat Mesra Alam untuk Ion Kalsium)

EMILY S MAJANUN[3,5], FATIN NUR AIN ABDUL RASHID[1], MUHAMAD KAMIL YAAKOB[2,4], AHMAD SAZALI HAMZAH[1], ZURINA SHAAMERI[1], KARIMAH KASSIM[1,3], NOOR HIDAYAH PUNGOT[1,3], MUHAMAD AZWAN HAMALI[3], AHMAD SHALABI MD SAURI[5], FARHANA JAAFAR AZUDDIN[5], YON AZWA SAZALI[5], M ZUHAILI KASHIM[5] & MOHD FAZLI MOHAMMAT[1,3]

[1]*Centre of Chemical Synthesis & Polymer Technology, Institute of Science, Universiti Teknologi MARA Puncak Alam, 42300 Puncak Alam, Selangor, Malaysia*
[2]*Centre of Functional Materials & Nanotechnology, Institute of Science, Universiti Teknologi MARA Shah Alam, 40450 Shah Alam, Selangor, Malaysia*
[3]*School of Chemistry and Environment, Faculty of Applied Sciences, Universiti Teknologi MARA Shah Alam, 40450 Shah Alam, Selangor, Malaysia*
[4]*School of Physics and Material Studies, Faculty of Applied Sciences, Universiti Teknologi MARA Shah Alam, 40450 Shah Alam, Selangor, Malaysia*
[5]*PETRONAS Research Sdn Bhd, Lot 3288 & 3289, Off Jln Ayer Itam, Kawasan Institusi Bangi, 43000 Kajang, Selangor, Malaysia*

Received: 31 May 2025/Accepted: 18 November 2025

ABSTRACT

Several chelating agents, including amine diacetic acid and amino acid diacetic acid, have been synthesized for the purpose of treating and controlling unwanted metal cations applications, specifically targeting divalent ions such as calcium (Ca^{2+}) that contribute to scale formation in high temperature carbonate environments. To evaluate their effectiveness, Density Functional Theory (DFT) calculation was performed to assess electronic reactivity through quantum descriptors including EHOMO, ELUMO, energy gap (ΔE), electron affinity (A), ionization potential (I), electronegativity (χ), global hardness (η), and global softness (σ). A diacetic acid (ADA) exhibited the lowest HOMO-LUMO energy gap, indicating high molecular reactivity toward metal surfaces. Monte Carlo simulations were conducted to determine the most stable adsorption configurations and quantify the adsorption energies of each chelating agent with Ca^{2+} ions. The ranking of adsorption affinity was found to be: GlnDA > ADA > PDA > BnDA > EDA > BDA, with GlnDA exhibited the highest adsorption energy, suggesting strong adsorption towards Ca ions. In reality, performance study conducted demonstrates that GlnDA exhibits a notable ability to dissolve Ca from carbonate rock under acidic conditions.

Keywords: Adsorption energy; calcite dissolution; calcium ions; chelating agent; density functional theory (DFT); Monte Carlo simulation

ABSTRAK

Beberapa agen pengkelat, termasuk asid diasetik amina dan asid diasetik berasaskan asid amino, telah disintesis bagi tujuan merawat dan mengawal aplikasi kation logam yang tidak diingini, khususnya mensasarkan ion dwivalen seperti kalsium (Ca^{2+}) yang menyumbang kepada pembentukan kerak dalam persekitaran karbonat bersuhu tinggi. Bagi menilai keberkesanan agen ini, pengiraan Teori Fungsi Ketumpatan (DFT) telah dijalankan untuk menilai kereaktifan elektronik melalui parameter global kuantum seperti EHOMO, ELUMO, jurang tenaga (ΔE), pertalian elektron (A), potensi ionisasi (I), elektronegatif (χ), kekerasan global (η) dan kelembutan global (σ). Simulasi Monte Carlo dilakukan bagi mengenal pasti konfigurasi dan penjerapan tenaga yang paling stabil untuk mengkelat ion kalsium (Ca^{2+}), kedudukan penjerapan tenaga adalah seperti berikut: GlnDA > ADA > PDA > BnDA > EDA > BDA. GlnDA menunjukkan penjerapan tenaga tertinggi, menandakan tahap penjeratan yang kuat terhadap ion kalsium. Secara realiti, kajian prestasi menunjukkan bahawa GlnDA berkebolehan untuk melarutkan kalsium daripada batuan karbonat dalam keadaan berasid.

Kata kunci: Agen pengkelat; ion kalsium; pelarutan kalsit; simulasi Monte Carlo; tenaga penjerapan; teori fungsi ketumpatan

INTRODUCTION

Chelating agents are compounds that can control the unfavourable reactions of metal ions in various applications (Fredd & Fogler 1998; Knepper 2003). They are used to prevent metal precipitation, remove scale from the systems, and as stimulation fluids (Hassan et al. 2020; Mahmoud 2018; Mahmoud & Nasr-El-Din 2014; Repo et al. 2013). Aminopolycarboxylic acid (APCA) is a type of chelating agent that typically contains one or more nitrogen atoms bonded to carbon atoms with multiple carboxyl groups (Muhammad Haziq et al. 2022; Repo et al. 2013). APCA can form stable metal complexes by chelating with metal ions *via* two or more separate dative bonds (Mahmoud et al. 2011). For instance, ethylenediaminetetraacetic acid (EDTA) can bind to metals such as Fe and Ca *via* six dative bonds, which are four carboxyl and two amine groups (Mahmoud et al. 2011).

In the oil and gas industry, chelating agents are used in stimulation acids to treat or remove scales that are formed on the oil well surface. Some examples of scales are carbonates (Ca, Mg, and Fe(II)), silicates (Ca, Na, Mg, and Al), sulphides (Fe(II) and Zn), oxides and hydroxides (Mg, Fe(II), and Fe(III)) (Frenier 2001). Common APCA chelating agents that have been used in the industry are EDTA, glutamic acid diacetate (GLDA), hydroxylethylene diamine triacetic acid (HEDTA), diethylene triamine pentaacetic acid (DTPA), ethanoldiglycinic acid (EDG), and nitrilotriacetic acid (NTA) (Frenier 2001; Frenier et al. 2003, 2000; LePage et al. 2011). Major problems with most of these chelating agents are their limited dissolving power and negative environmental impact (Mahmoud et al. 2011). For example, EDTA and DTPA have low solubility in hydrochloric acid (HCl) and are not biodegradable, while NTA is acid soluble and biodegradable but has a lower stability constant for iron and is carcinogenic to animals (Mahmoud et al. 2011). GLDA, on the other hand, has good solubility in HCl, is readily biodegradable, and is very effective in dissolving calcium carbonate ($CaCO_3$) as compared to other chelating agents (LePage et al. 2011).

To ensure optimal interaction between chelating agents and a metal surface, the chelating agents must possess heteroatoms that are abundant with free lone pair electrons (e.g., nitrogen (N), oxygen (O), sulphur (S), phosphorus (P)) and/or aromatic ring with *p*-electrons. The heteroatoms and aromatic ring can achieve major chemical adsorption *via* electron transfer between the additive and the metal. Therefore, we synthesized several chelating agents that are rich in O and N atoms, inspired by the structures of commercial chelating agents like GLDA, HEDTA, and EDG (Frenier 2001; Frenier et al. 2003, 2000; LePage et al. 2011). The 'claw' or two negatively charged carboxyl groups (COOH) were installed at the N atom of amine and amino acid as the starting materials.

In this article, the quantum chemistry and adsorption energy of the synthesized chelating agents towards Ca ion were investigated using computational methods based on DFT and Monte Carlo approaches. The molecular structure of the synthesized chelating agents was optimized by quantum chemical calculation (Muhammad Haziq et al. 2022; Obot et al. 2016). The value of the energy gap reflects the reactivity of chelating agents (Miar et al. 2021; Pilli, Banerjee & Mohanty 2015). The electron density of the atomic surface reflects the active site of the reaction (Xu et al. 2018). The adsorption of molecules on metal surfaces was calculated by molecular dynamic simulation (Singh et al. 2019). The adsorption and binding energy values reflect the chelating ability.

The purpose of insertion of carbonyl groups (-COOH) was selected due to their ability to serve as robust coordination sites for metal cations via oxygen lone pairs. These groups easily deprotonate in mildly acidic to neutral circumstances, producing negatively charged carboxylates ($-COO^-$) that can form stable five or six membered chelate rings with divalent ions like Ca^{2+} (Bucheli-Witschel & Egli 2001). In aminopolycarboxylic acid (APCA) systems, donor atoms interact with nitrogen donors to improve thermodynamics stability and complexation kinetics, a characteristic well-documented in EDTA, GLDA and HEDTA systems (Hassan, Mahmoud & Patil 2021; Mahmoud et al. 2016). Thus the -COOH group are recognised as critical for optimising the binding efficiency of Ca^{2+} ions, facilitating stronger interactions necessary for various application in environmental and industrial context (Dong et al. 2023; Mahmoud 2018).

The way that chelating agents and metal ions bind together usually involves coordinate covalent bonds between nitrogen and oxygen donor atoms. The lone pairs from these atoms mix with the empty orbitals of divalent cations to make stable five- to six-membered chelate rings. This dual donor mechanism increases the stability of the complex by using both covalent and electrostatic attraction. Previous DFT and NMR investigations (Mahmoud et al. 2011; Muhammad Haziq et al. 2022) have substantiated that these interactions are primarily governed by N→M and O→M coordination, leading to mixed ionic – covalent metal – ligand bonds crucial for the formation of stable complexes.

MATERIALS AND METHODS

GENERAL DETAILS

All reagents were supplied by Merck Chemical Co., Sigma-Aldrich Co., and Acros Organics Co., and used without additional purification. NMR spectra were recorded on JEOL Resonance ECZ400 [400 MHz (^1H) and 100 MHz (^{13}C)] using TMS as the internal standard. The progress of the reactions was monitored by thin-layer chromatography (TLC) on silica gel 60 F254 and the spots were visualized with the UV lamp (254 and 365 nm). Thermogravimetric analysis (TGA) was carried out using Perkin-Elmer TGA8000 with a heating rate at 10 ºC/min, and nitrogen flow at 20 mL/min.

SYNTHESIS OF AMINE DIACETIC ACID (1-5)

Amine (1.0 mmol), KOH (5.0 mmol), and 2-chloroacetic acid (2.5 mmol) were refluxed in H_2O (10 mL) as a green solvent for 4 h (Figure 4). After being cooled down, the mixture was acidified with 6M HCl, and the mixture was evaporated under reduced pressure. The solid was washed with MeOH and filtered. The filtrate was rotavaped to get the white solid as the diacetic acid product in high yield (81-91%). No column chromatography was involved during the purification process.

Ethylamine diacetic acid (EDA) (1) White solid, Yield: 89%. ^{1}H-NMR (400 MHz, D_2O) δ 3.79 (s, 4H), 3.16 (q, J = 7.3 Hz, 2H), 1.08 (t, J = 7.3 Hz, 3H). ^{13}C-NMR (101 MHz, D_2O) δ 169.5 (C=O), 55.3 (2 × CH_2COOH), 52.0 (CH_2), 8.8 (CH_3).

Propylamine diacetic acid (PDA) (2) White solid, Yield: 91%. ^{1}H-NMR (400 MHz, D_2O) δ 3.83 (s, 4H), 3.19 (t, J = 8.0 Hz, 2H), 1.71 (td, J = 15.1, 7.5 Hz, 2H), 0.94 (t, J = 7.3 Hz, 3H). ^{13}C-NMR (101 MHz, D_2O) δ 170.4 (C=O), 58.0 (CH_2), 56.8 (2 × CH_2COOH), 17.6 (CH_2), 10.1 (CH_3).

Butylamine diacetic acid (BDA) (3) White solid, Yield: 87%. ^{1}H-NMR (400 MHz, D_2O) δ 3.72 (s, 4H), 3.03-2.97 (m, 2H), 1.42-1.34 (m, 2H), 1.06 (td, J = 14.8, 7.5 Hz, 2H), 0.60 (t, J = 7.5 Hz, 3H). ^{13}C-NMR (101 MHz, D_2O) δ 168.2 (C=O), 55.3 (CH_2), 54.5 (2 × CH_2COOH), 24.4 (CH_2), 18.0 (CH_2), 11.6 (CH_3).

Benzylamine diacetic acid (BnDA) (4) Dark green solid, Yield: 86%. ^{1}H-NMR (400 MHz, CD_3OD) δ 7.53-7.47 (m, 5H), 4.57 (s, 2H), 4.17 (s, 4H). ^{13}C-NMR (101 MHz, CD_3OD) δ 166.9 (C=O), 131.5 (CHAr), 130.4 (CHAr), 129.1 (CHAr), 128.3 (quart. ArC), 59.1 (CH_2), 52.9 (2 × CH_2COOH).

Aniline diacetic acid (ADA) (5) White solid, Yield: 81%. ^{1}H-NMR (400 MHz, D_2O) δ 6.62-6.58 (m, 2H), 6.14 (t, J = 7.3 Hz, 1H), 5.92 (d, J = 7.8 Hz, 2H), 3.48 (s, 4H). ^{13}C-NMR (101 MHz, D_2O) δ 177.0 (C=O), 146.0 (quart. ArC), 129.2 (CHAr), 117.7 (CHAr), 111.1 (CHAr), 54.0 (2 × CH_2COOH).

SYNTHESIS OF GLUTAMINE DIACETIC ACID, GlnDA (6)

Glutamine (171 mmol) and KOH (171 mmol) were stirred in 425 mL of distilled water until all the reagents were dissolved. In another flask, chloroacetic acid (342 mmol) was dissolved with distilled water (100 mL) and was cautiously added KOH (342 mmol). While stirring, the chloroacetic acid potassium solution was added dropwise to the glutamine potassium solution. The mixture was heated at 60-70 °C for 4 h. The pH was kept between 10 and 11 by dosing 50% KOH solution. The mixture was rota-vaped to get the white solid. The solid was washed with methanol to get the GDA in 87% yield. No column chromatography was involved during the purification process.

Glutamine diacetic acid (GlnDA) (6) Colourless oil. Yield: 87%. ^{1}H-NMR (400 MHz, D_2O) δ 3.64-3.58 (m, 1H), 3.44 (s, 2H), 3.41 (s, 2H), 1.85-1.76 (m, 1H), 1.70-1.65 (m, 2H), 1.48-1.36 (m, 1H). ^{13}C-NMR (101 MHz, D_2O) δ 177.2 (C=O), 176.2 (C=O), 173.0 (C=O), 59.0 (2 × CH_2COOH), 56.1 (CH), 28.8 (CH_2), 24.1 (CH_2).

QUANTUM CHEMICAL CALCULATION

The quantum chemical calculation of the proposed chelating agents was carried out using the DMol^3 module of Material Studio software as available in BIOVIA Inc (Delley 2000, 1990). The structure of all compounds in the gas phase were optimized using the B3LYP hybrid functional within the DFT framework (Becke 1993; Stephens et al. 1994). The double numerical with polarisation (DNP) function was used as a basis set (Delley 2000). DNP is identified as the basis set which is comparable to the 6-31G++(d,p) Gaussian basis set (Benedek et al. 2005) because it is more stable and works better for medium sized organic molecules in DFT geometry optimisations, especially in condensed-phase systems. DNP does not use diffuse functions which can cause problems with convergence on large molecular surfaces like chelating agents.

In all geometric optimizations, the convergence energy tolerance of 1.0×10^{-5} Ha, the maximum force of 0. 002 Ha/Å, and the maximum displacement of 0. 005 Å were used. The quantum global parameters, such as energy gap (ΔE), electron affinity (A), ionisation potential (I), electronegativity (χ), global hardness (η) and global softness (σ) were calculated using the following equations:

$$\Delta E = E_{LUMO} - E_{HOMO} \quad (1)$$

$$A = -E_{LUMO} \quad (2)$$

$$I = -E_{HOMO} \quad (3)$$

$$\chi = (I + A)/2 \quad (4)$$

$$\eta = (I - A)/2 \quad (5)$$

$$\sigma = 1/\eta \quad (6)$$

MOLECULAR DYNAMICS SIMULATION

The molecular dynamics calculation of the proposed chelating agents' adsorption toward Ca ion was performed by Adsorption Locator module within the Material Studio software (Frenkel & Smit 1996). Theoretically, quantum chemical calculation was used to explore the molecular structures of the chelating agents and their interactions with metal cation. The Monte Carlo (MC) search was used to calculate the low configuration adsorption energy. The adsorption locator is essentially a simulated annealing

simulation with geometry optimizations in between successive heat-cool cycles where a temperature is applied and decreases gradually (Frenkel & Smit 1996; Metropolis et al. 1953). The isosteric heat, or enthalpy of adsorption, can be extracted from the adsorption calculation and is an average overall the lowest energy configurations returned after each annealing cycle of the molecular dynamics run. Five cycles containing 50 000 steps per cycle with annealing temperatures of 1.0×10^{-5} to 100 K were used. The Monte Carlo parameters were set to a probability of 0.32 (ratio = 1) for 'conformer', 'rotate' and 'translate' while 'regrow' was set to 0.03 (ratio = 0.1). The Universal force field was used with group based and atomic based summation methods for the electrostatic and van der Waals energy components, respectively, with the cut-off's set at 15.5 Å (Casewit, Colwell & Rappe 1992a, 1992b; Rappe, Colwell & Casewit 1993; Rappe et al. 1992).

DISSOLUTION OF CALCITE

The outcrop limestone cores were crushed and sieved to obtain the calcite ($CaCO_3$) powder with particle sizes of 90-125 μm. The powder was oven-dried overnight before use. The chelators were prepared at 20 wt.% concentration. Hydrochloric acid (HCl) was added to recondition the earlier-mentioned chelators at pH 3. Calcite/chelator with a molar ratio of 1:5 was added to the digestion tube at 90 °C. The samples were removed at set time periods and filtered using the filter paper. The clear filtrate was analysed for total Ca concentration by using inductively coupled plasma(ICP) spectroscopy.

RESULTS AND DISCUSSION

The results and discussion chapter are divided into five different sections. The first section discussed the synthesis of the green chelating agents. The second section described the quantum chemical study of the synthesized chelating agents. The third section deals with the adsorption energy of the synthesized chelating agents towards the Ca ion. The fourth section discussed the dissolution of calcite by the synthesized chelating agents. Finally, the thermal stability of the synthesized chelating agents is discussed in the fifth section.

SYNTHESIS

The synthesis of the chelating agents (**1**–**6**) was carried out *via* an *N*-alkylation reaction of amines (ethylamine, propylamine, butylamine, benzylamine, and aniline) and amino acid (glutamine) by installing two negatively charged carboxyl groups (COOH) or the 'claw' at the N atom. By refluxing amine, potassium hydroxide, and 2-chloroacetic acid as a source of the 'claw', amine diacetic acid dipotassium salt was obtained. Amine diacetic acid dipotassium salt was then acidified to yield amine diacetic acid (**1**–**5**) in good yield without the purification process. The structure of compounds **1**–**5** was confirmed by the appearance of one sharp singlet peak for CH_2 of the 'claw' in the ^{1}H NMR and ^{13}C NMR spectra. The structures of **1**–**5** was consistent with the previous report as the synthetic route is based on the classical *N*-alkylation of amines with chloroacetic acid in an alkaline aqueous environment. This was first reported by Ziemlak et al. (1950) and later improved for different substituted amines (Fujieda, Maeda & Kato 2018; Hijazi et al. 2018; Mandava et al. 2017; Ziemlak et al. 1950).

For amino acid diacetic acid, GlnDA (**6**), the reaction was prepared using the same method as above by heating glutamine, 2-chloroacetic acid, and potassium hydroxide in water (Scheme 2). GlnDA (**6**) was obtained in good yield without any purification process (Tuerk et al. 2019). Interestingly, the reaction for compounds **1**–**6** can be adopted for a large-scale setup (up to 5 L) by employing the same equivalent reaction.

Using the same molar ratios, the optimized synthetic protocol was successfully scaled up to a 5 L reaction volume, and the yields for all derivatives stayed between 81% and 91%. The scalability shows that the reaction is strong, which shows that it can be used to make semi-industrial products in a safe, mild and green-solvent environment.

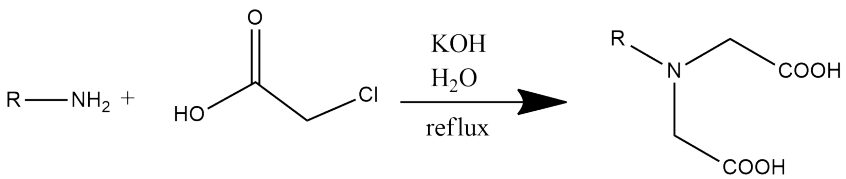

1. R = CH_3CH_2
2. R = $CH_3CH_2CH_2$
3. R = $CH_3CH_2CH_2CH_2$
4. R = Bn
5. R = Ph

SCHEME 1. Synthesis of amine diacetic acid (**1**–**5**)

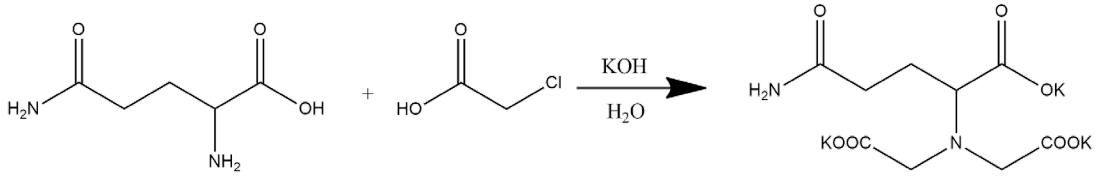

SCHEME 2. Synthesis of GlnDA (**6**)

QUANTUM CHEMICAL STUDY

Having successfully synthesized the chelating agents (**1**–**6**), the simulation study towards the quantification performance of the compounds was performed. The molecular structure and energy optimization of the chelating agents can be obtained by quantum chemical calculation. Based on the frontier molecular orbital theory, the chemical reactivity of the chelating agents was associated with the highest occupied molecular orbital (HOMO) and the lowest unoccupied molecular orbital (LUMO). The HOMO is related to the nucleophilic or electron-donating, while the LUMO is referred to the electrophilic or electron-accepting.

Table 1 lists the molecular orbital distribution and possible reactive sites of the commercial chelating agents (GLDA, HEDTA, and EDG) and synthesized chelating agents (**1**–**6**). It can be seen from Table 1 that the HOMO of all the chelating agents is mainly distributed on the amine group, while the LUMO is mainly distributed on the carboxylic acid group. However, the LUMO distribution is not evenly distributed among the four oxygen of the 'claw'. The results of the molecular orbital distributions indicate the chelating agents can donate the electrons from the nitrogen atom to the empty orbital of the Ca ion to form a dative bond. Meanwhile, the oxygen atom can accept the electrons from the Ca ion to form a feedback bond.

Table 2 shows the quantum chemical calculation parameters of the chelating agents. By using the HOMO and LUMO energies, important properties like electron affinity (A), ionisation potential (I), electronegativity (χ), global hardness (η), and global softness (σ) were calculated. The theoretical backgrounds of the mentioned properties are described herewith. The energy difference between the HOMO and LUMO is defined as the energy gap (ΔEgap). The energy gap (ΔE) reflects the strength, stability, and chemical reactivity of the compound (Noureddine et al. 2021; Xu et al. 2018). A molecule with a low ΔEgap value is less stable and more reactive because it is easier for the electron to flow from low-lying HOMO to high-lying LUMO (Miar et al. 2021; Noureddine et al. 2021). From Table 2, it can be observed that ADA (5) has the lowest ΔEgap value, which indicates the compound gives better adsorption properties and easier chelation reaction towards Ca ion as compared to the commercial chelating agents (GLDA, HEDTA, and EDG).

The difference in the lengths and types of R-groups also plays a significant role in modulating orbital energies and electron distribution. Longer alkyl chains, such as those in BDA (3) and PDA (4), exhibit weak inductive electron-donating effects (+I), which raise the HOMO energy and enhance nucleophilicity. This facilitates electron donation to Ca^{2+} ions. In contrast, aryl substitution in ADA (5) introduces a π-system that withdraws electron density (–I effect), stabilizing the LUMO and lowering ΔEgap. This electronic modulation directly influences adsorption behavior: electron-donating groups promote electron transfer to Ca^{2+}, while electron-withdrawing groups improve orbital overlap and strengthen overall binding affinity.

The electron affinity (A) and ionisation potential (I) are related to the molecule's ability to withdraw or donate the electron, respectively (Yusuf et al. 2021). The A is defined as the amount of energy liberated when an electron is added to a neutral atom to form a negatively charged ion (Muhammad Haziq et al. 2022). The more negative the A value, the more favourable the addition of the electron (Muhammad Haziq et al. 2022). Thus, it is evident from Table 2 that BDA (3) is the easiest to accept the electron to form a negative ion. On the other hand, the I is defined as the amount of energy required to remove an electron from an atom. In general, the lower the I value, the higher the reactivity of the compound towards metal cation (Al Hamad et al. 2020). Hence, it is suggested that ADA (5) requires the least amount of energy to remove the electron from the molecule, which accounts for the high reactivity itself.

Electronegativity (χ) and global hardness (η) are associated with the A and I values. The χ indicates the tendency of molecules to attract the electron. It is noted that compound with high χ value is difficult to give their electrons (Obot et al. 2016; Pilli, Banerjee & Mohanty 2015). Considering the result in Table 2, it was found that ADA (5) has the lowest χ value (5.719eV), suggesting the compound is more reactive towards metal cation compared to the other chelating agents.

Global hardness (η) and global softness (σ) are indications of the polarizabilities of the molecules and reflect the molecular flexibility (Obot et al. 2016; Pilli, Banerjee, and Mohanty 2015; Singh et al. 2019; Yusuf et al. 2021). Thus, it can be noted that molecule with higher η value is very stable and are not favourable towards metal cation (Obot et al. 2016; Pilli, Banerjee & Mohanty 2015). On the contrary, global softness (σ) is the reciprocal of the global hardness; in other term, a molecule with a high σ value has good chelation with the metal cation

TABLE 1. The molecular orbital distribution and possible reactive sites of the commercial chelating agents (GLDA, HEDTA, and EDG) and synthesized chelating agents (**1**–**6**)

Chelating agent	Number of atoms (active sites)	Optimized structure	HOMO	LUMO
GLDA	N = 1, C = 9, O = 8, H = 13, 31 atoms	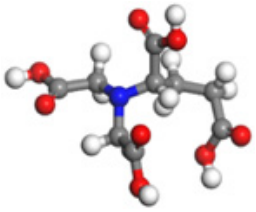	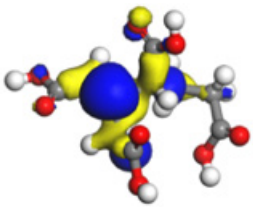	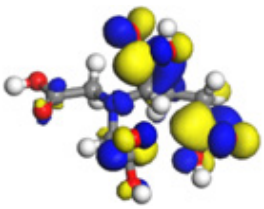
HEDTA	N = 2, C = 10, O = 7, H = 18, 37 atoms	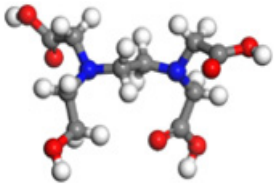	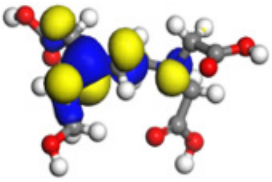	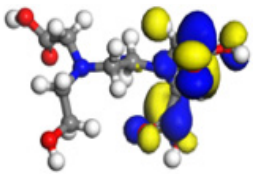
EDG	N = 1, C = 6, O = 5, H = 11, 23 atoms	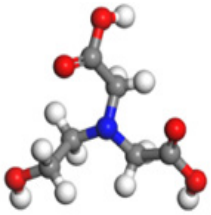	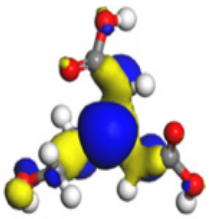	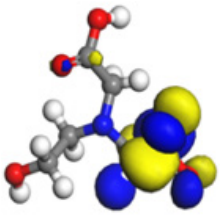
EDA (**1**)	N = 1, C = 6, O = 4, H = 11, 22 atoms	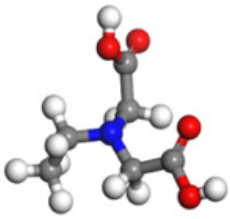	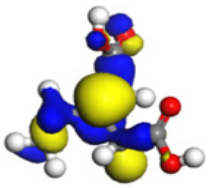	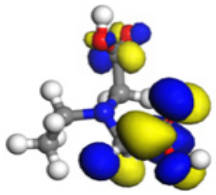
PDA (**2**)	N = 1, C = 7, O = 4, H = 13, 25 atoms	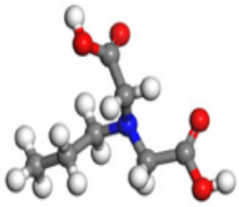	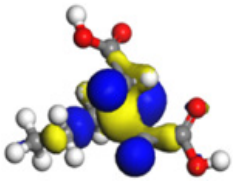	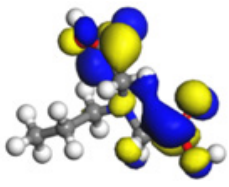
BDA (**3**)	N = 1, C = 8, O = 4, H = 15, 28 atoms	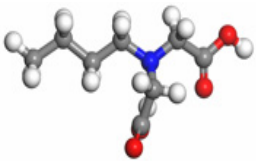	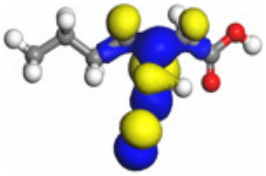	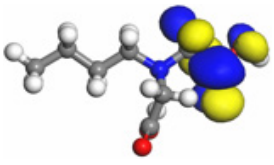

continue to next page

continue from previous page

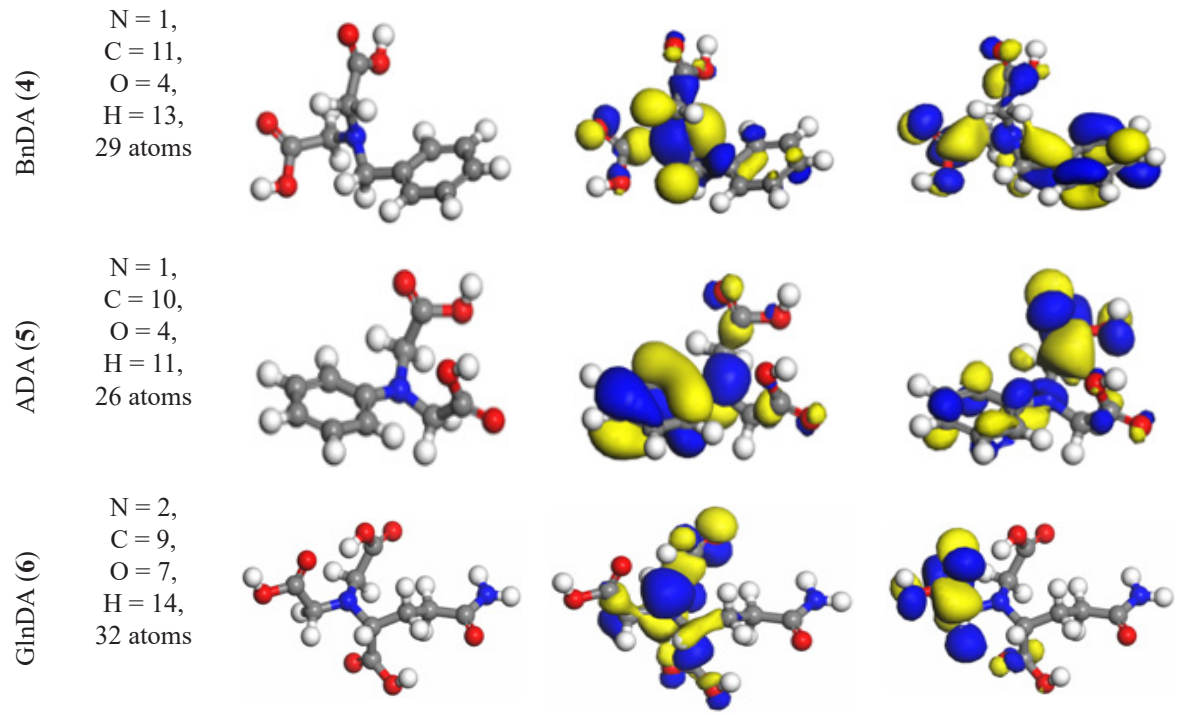

TABLE 2. Quantum properties of the commercial and synthesized chelating agents (**1**–**6**)

Chelating Agents	E_{HOMO}	E_{LUMO}	Energy Gap, ΔE	Electron Affinity, A	Ionization Potential, I	Electronegativity, χ	Global Hardness, η	Global Softness, σ
	eV							
GLDA	-6.212	-0.127	6.085	0.127	6.212	3.170	3.043	0.329
HEDTA	-5.599	-0.046	5.553	0.046	5.599	2.823	2.777	0.360
EDG	-6.333	0.055	6.388	-0.055	6.333	3.139	3.194	0.313
EDA (**1**)	-6.150	-0.222	5.928	0.222	6.150	3.186	2.964	0.337
PDA (**2**)	-6.211	-0.217	5.994	0.217	6.211	3.214	2.997	0.334
BDA (**3**)	-6.440	0.021	6.461	-0.021	6.440	3.210	-3.231	-0.310
BnDA (**4**)	-6.338	-0.531	5.807	0.531	6.338	3.435	2.904	0.344
ADA (**5**)	-5.238	-0.059	5.179	0.059	5.238	2.649	2.590	0.386
GlnDA (**6**)	-6.890	-0.924	5.966	0.924	6.890	3.907	-2.983	-0.335

(Attia, Elgendy & Rizk 2019; Guo et al. 2017). Thus, it can be seen from Table 2 that BDA (3) is the least stable, which means the compound is more reactive towards metal cation as compared to other chelating agents.

ADSORPTION ENERGY

The adsorption energy is energy required for the chelating agent to move towards the metal cation (Ding et al. 2020; Obot et al. 2016). On the other hand, the binding energy

($E_{binding}$ = -$E_{adsorption}$) is the force between the chelating agent and the metal cation (Ding et al. 2020; Guo et al. 2017). Generally, the lower (more negative value) the adsorption energy value, the easier it is for the chelating agent to chelate with the metal cation. Conversely, the greater the binding energy value, the stronger the binding force between the chelating agent and the metal cation (Ding et al. 2020; Guo et al. 2017; Obot et al. 2016).

Table 3 presents the calculated adsorption and binding energies of the commercial and synthesized chelating agents (**1**–**6**) towards Ca ion. The adsorption energy was calculated using Monte Carlo simulation. The negative value of adsorption energy indicates the adsorption process could occur spontaneously (Ding et al. 2020; Obot et al. 2016). It should be emphasized that the adsorption energy calculation is computed at a ground-state environment and in vacuum conditions. Therefore, factors such as concentration, kinetic energy, environment, and pH-dependent solubility are not included in the calculation. Despite that, the calculated adsorption energy can provide crucial information for predicting adsorption energy.

From Figure 1, the adsorption energy of the synthesized chelating agents on Ca ion decreased in the following order: GlnDA (**6**) > ADA (**5**) > PDA (**2**) > BnDA (**4**) > EDA (**1**) > BDA (**3**) with value of GlnDA (6) = -48.14 kcal/mol, ADA (5)=-39.09 kcal/mol, PDA (2) =38.25 kcal/mol, BnDA (4) = -36.45 kcal/mol, EDA (1) = -33.92 kcal/mol, BDA (3)=-30.95 kcal/mol. This order indicates that the adsorption of GlnDA (**6**) towards Ca ion is strong, stable, and spontaneous. GlnDA (**6**) also gives the maximum binding energy, which indicates that the compound will adsorb strongly towards Ca ion and has better chelation performance than the other proposed chelating agents.

DISSOLUTION OF CALCITE

Upon having the highest adsorption energy as compared to other synthesized chelating agents, the dissolution test of GlnDA (**6**) was conducted to determine its ability to dissolve the calcite. The test was carried out at pH 3 and at 90 ºC. The dissolution test was done at pH 3 to mimic the acidic conditions that are common in carbonate reservoirs where well-stimulation fluids are used. At this pH, the chelating agent partially protonates, giving off enough H+ to start a reaction with $CaCO_3$ on the surface while keeping the carboxylate functional groups intact for chelation. When the pH is higher, protons are less active and the process of dissolving is slower. When the pH is lower (less than 2), acid corrosion happens too quickly and without controlled complexation. So, pH 3 is the best balance between acid reactivity and chelation control. To maintain a constant molar ratio between the calcite and chelating agents, each sample was prepared and collected from a single test. The acid portion of the chelating agents was participated in the calcite ($CaCO_3$) dissolution:

$$2H^+ + CaCO_3 \rightarrow Ca^{2+} + CO_2 + H_2O$$

The dissolution capacity of GlnDA (**6**) was compared to the commercial chelating agents GLDA, HEDTA, and EDG. Figure 2 and Table 4 show the Ca concentration obtained from calcite dissolution by GlnDA (**6**), GLDA, HEDTA, and EDG. A similar trend for the dissolution profile graphs of GLDA, HEDTA, and EDG was reported in the previous reports (Frenier 2001; Mahmoud et al. 2011). As noted by the concentration of Ca, HEDTA showed the highest calcite dissolved compared to other chelating agents. Interestingly, GlnDA (**6**) showed comparable Ca concentration as the commercial chelating agent, HEDTA and GLDA. It is likely GlnDA (**6**) has the potential to be a good chelating agent towards Ca ion since it has comparable dissolving capacity as HEDTA and GLDA.

The structural effect on Ca^{2+} detection is clear in the way carboxyl and amine groups are arranged in space and how they contribute to the electronic structure. GlnDA (6) for instance has two amine sites and many carboxylate sites, which allows for multidentate binding that improves surface adsorption. ADA (5) also has an aromatic ring next to groups that give off electrons. This makes π–cation interaction stronger and makes the surface more attractive. These characteristics indicate that electronics delocalisation and donor group density are essential for the chelating agent's detection and interaction with Ca^{2+} ions.

THERMAL STABILITY

Thermogravimetric analysis (TGA) determines the temperature at which decomposition occurs for each chelating agent. The onset decomposition temperature provides insight into the suitability of certain chelating agents for application in high-temperature environments. Based on the thermogravimetric (TG) profile, only ADA (**5**) exhibits an onset decomposition temperature over 200 °C (Figure 3). The differential thermogravimetric (DTG) curve showed that the onset temperature for the first curve of ADA (**5**) is recorded at 227.6 °C. For the other chelating agents, it is observed that their decomposition profile starts as early as 50 °C, which is probably due to the moisture removal from the compounds. The weight percent of these areas is between 1.4-1.5 wt.% for BDA, EDA, and PDA.

To provide a more comprehensive comparison, the weight % of each chelating agent that underwent decomposition within the temperature range of 30-150 °C was quantitatively determined (Figure 4). Three chelating agents, EDA (**1**), BnDA (**4**), and ADA (**5**) have a weight loss of less than 10% when subjected to a temperature of 150 °C, suggesting their notable thermal stability and potential unsuitability for high-temperature environments (above 150 °C).

Figure 5 shows the wt.% decomposition of all the chelating agents at high-temperature environments (above 150 °C). The sequence of decomposition of the

TABLE 3. The adsorption and binding energies of the commercial and synthesized chelating agents (**1**–**6**) towards Ca ion

Chelating agents	Fully deprotonated structure's adsorption on Ca^{2+}	Adsorption Energy (Ca^{2+}) kcal/mol Eads = Etotal – (Echelant + Esurface);	Binding Energy (Ca^{2+}) kcal/mol Ebind = –Eads.
GLDA	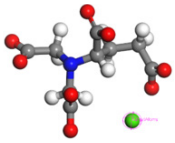	-71.380	71.380
HEDTA	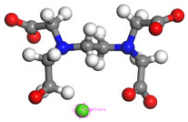	-62.611	62.611
EDG	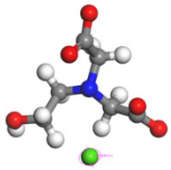	-36.031	36.031
EDA (1)	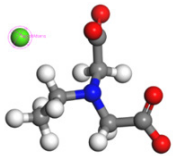	-33.923	33.923
PDA (2)	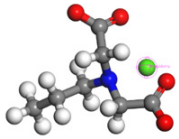	-38.248	38.248
BDA (3)	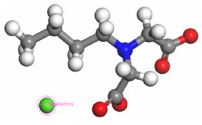	-30.947	30.947
BnDA (4)	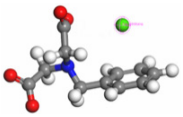	-36.448	36.448
ADA (5)	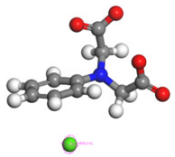	-.39.089	39.089
GlnDA (6)	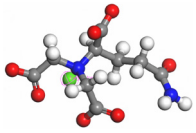	-48.142	48.142

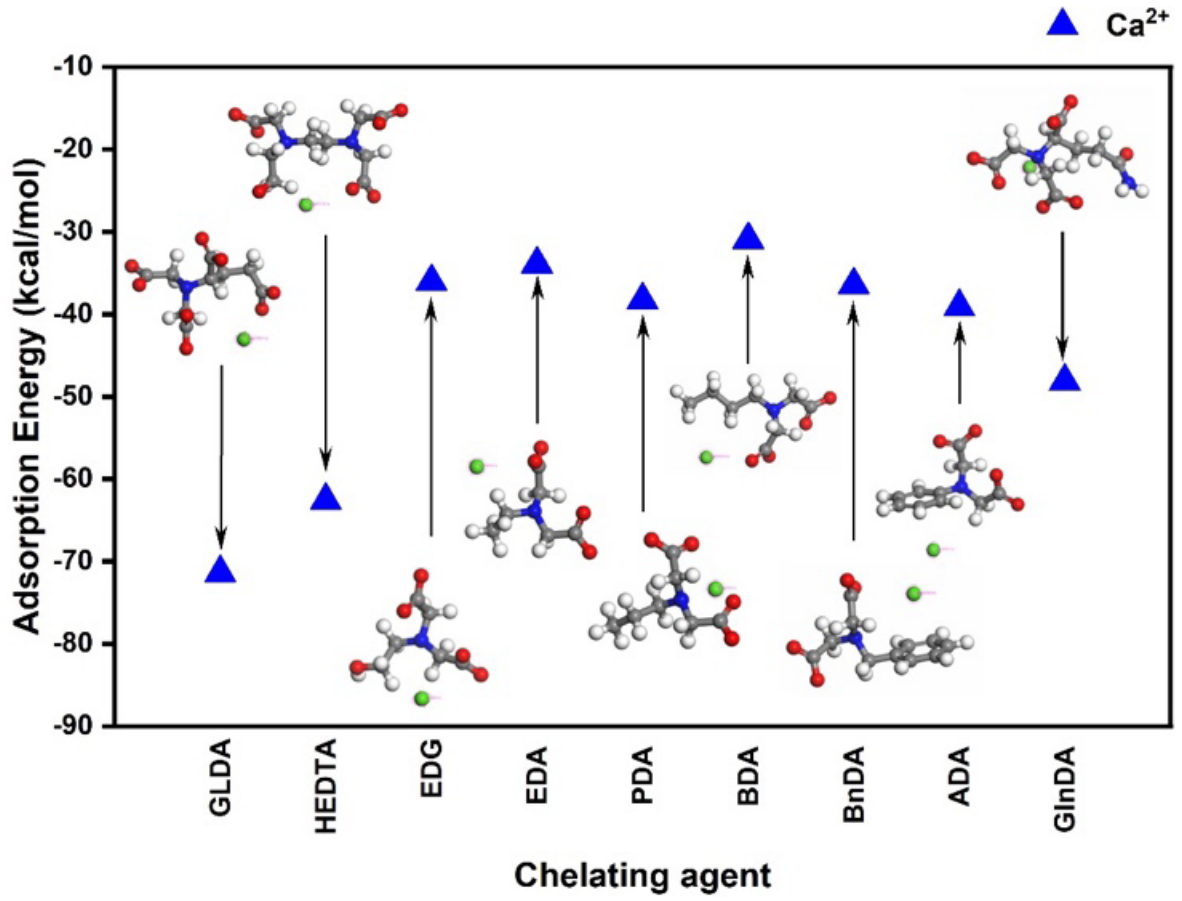

FIGURE 1. Calculated adsorption energy of the commercial and synthesized chelating agents (**1**–**6**) towards Ca ion

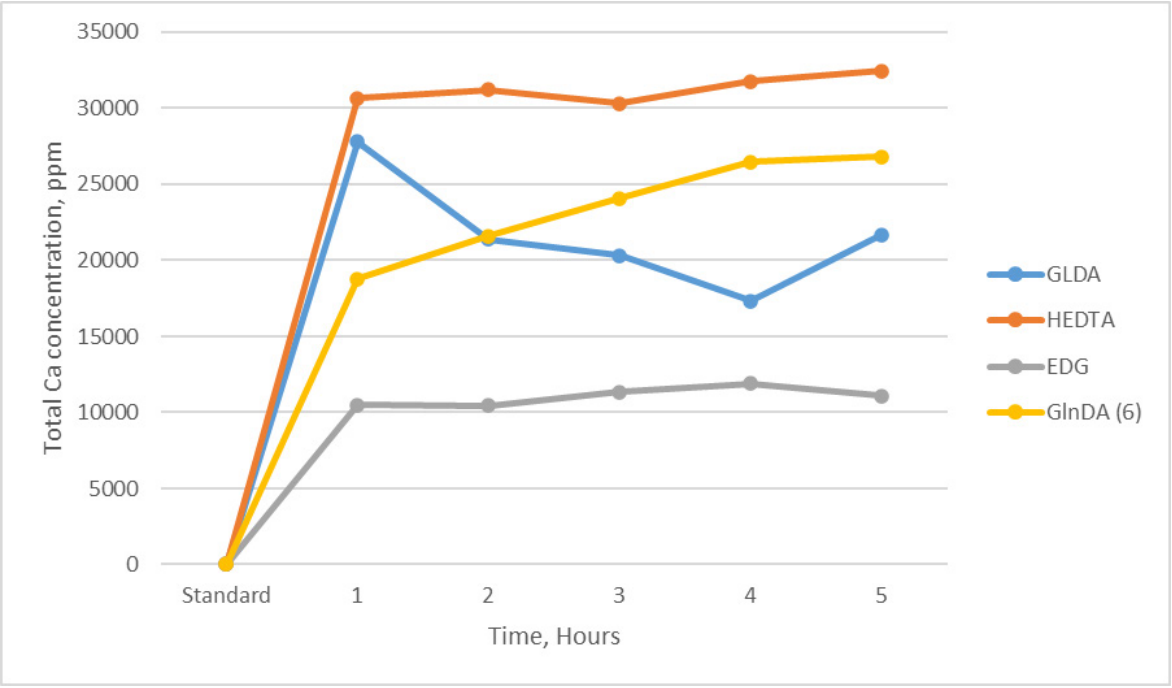

FIGURE 2. Dissolution of calcite by GlnDA (6), GLDA, HEDTA, and EDG at pH 3 at 90 ºC

TABLE 4. Summary of the results in Figure 2

Sampling Point (h)	Total Ca concentration (ppm)			
	GLDA	HEDTA	EDG	GlnDA (**6**)
Standard	0.00	0.00	0.00	0.00
1	27797.00	30660.00	10510.00	18765.40
2	21400.00	31210.00	10440.00	21616.50
3	20310.00	30310.00	11330.00	24083.60
4	17330.00	31750.00	11920.00	26451.30
5	21682.90	32470.00	11080.00	26810.00
6	15595.00	30090.00	11470.00	28951.00

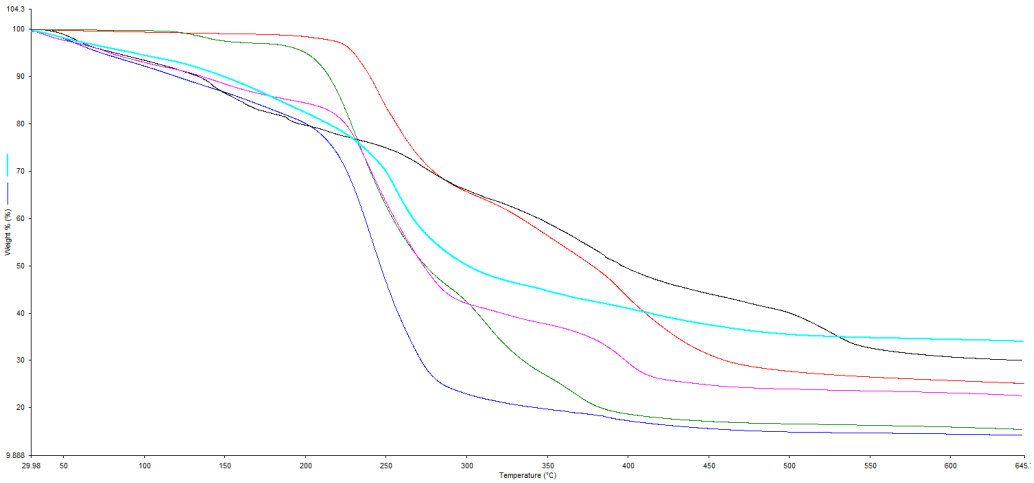

FIGURE 3. Thermal stability profile of synthesized chelating agents at elevated temperature

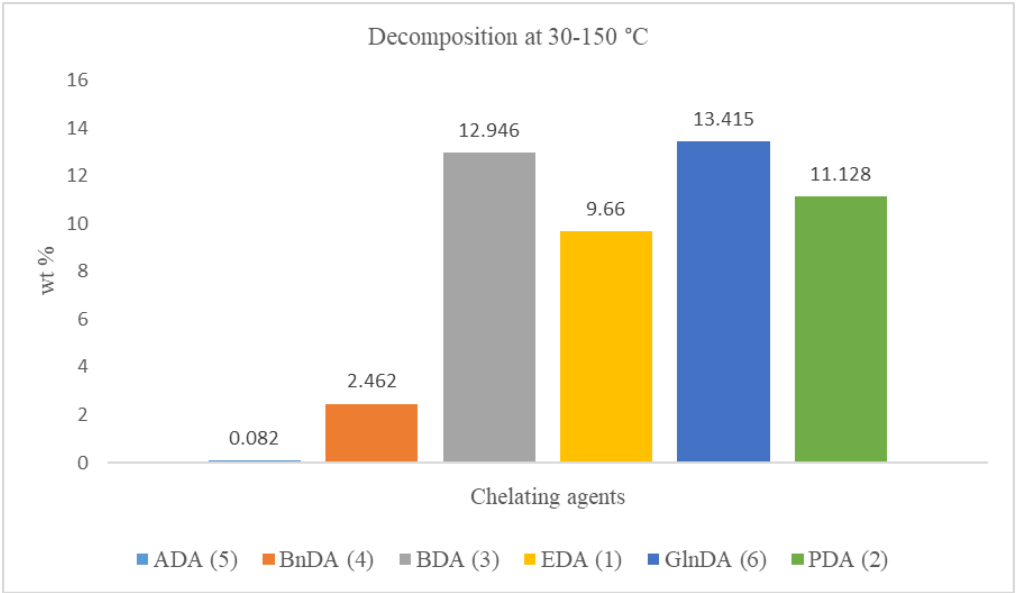

FIGURE 4. Wt.% decomposition of synthesized chelating agents at 30-150 °C

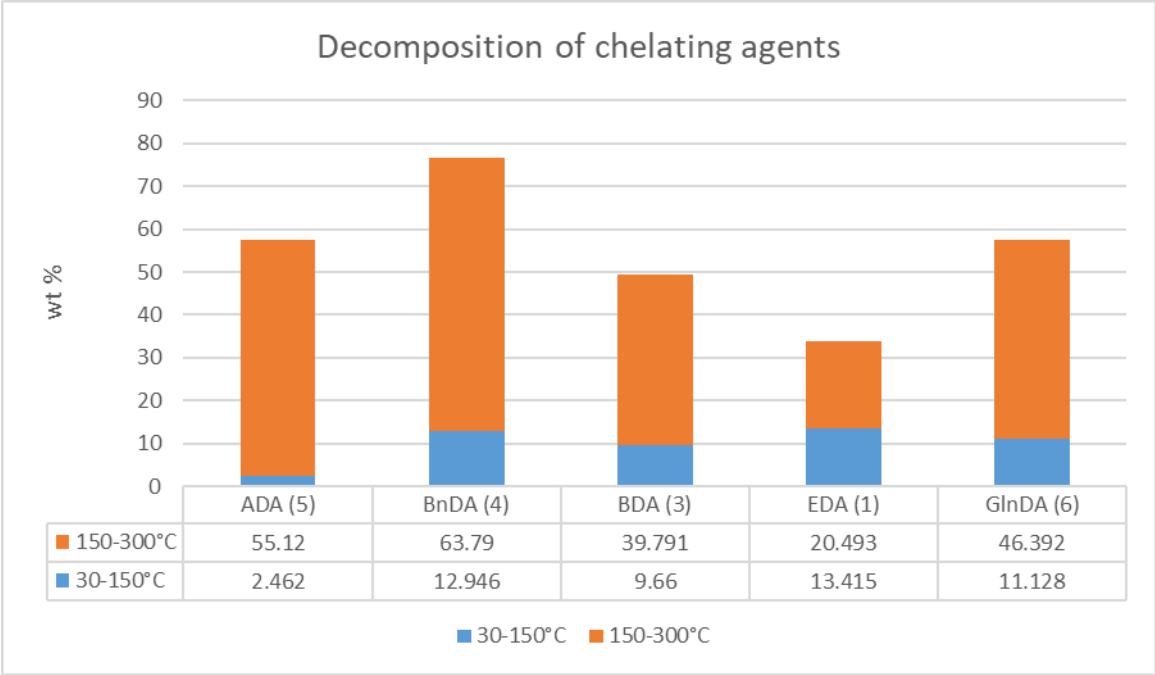

FIGURE 5. Wt% decomposition of synthesized chelating agents above 150 °C

chelating agents at high temperature is as follows, ranked from the most to the least decomposed: BDA (**3**) > BnDA (**4**) > PDA (**2**) > EDA (**1**) > ADA (**5**) > GlnDA (**6**). This wt.% decomposition could indicate the ability of the chelating agents to chelate with Ca ion at high temperature. This means that GlnDA (**6**) has a higher ability to chelate with Ca ion as compared to other synthesized chelating agents.

CONCLUSIONS

Six environmentally friendly chelating agents were synthesized by introducing carboxyl groups to improve metal ion coordination. Among them, GlnDA (**6**) demonstrated the highest theoretical binding affinity and strong experimental performance in dissolving calcite, comparable to standard agents like HEDTA and GLDA. A strong correlation was observed between computational predictions and experimental outcomes, validating the accuracy of the applied DFT and Force Field methods. However, GlnDA (**6**) showed lower thermal stability, indicating a need for structural enhancement to withstand high-temperature conditions. This study highlights a novel approach that integrates computational and experimental evaluation to guide the development of efficient and eco-friendly chelating agents.

ACKNOWLEDGEMENTS

We would like to extend our deep appreciation and gratitude to PETRONAS for its financial support [No.: 100-TNCPI/PRI 16/6/ 2 (058/2020)]; Universiti Teknologi MARA and PETRONAS Research Sdn. Bhd. for their support to this work in terms of instruments used for the experiments.

REFERENCES

Al Hamad, M., Al-Sobhi, S.A., Onawole, A.T., Hussein, I.A. & Khraisheh, M. 2020. Density-functional theory investigation of barite scale inhibition using phosphonate and carboxyl-based inhibitors. *ACS Omega* 5: 33323-3328. https://doi.org/10.1021/acsomega.0c05125

Attia, S.K., Elgendy, A.T. & Rizk, S.A. 2019. Efficient green synthesis of antioxidant Azacoumarin dye bearing spiro-pyrrolidine for enhancing electro-optical properties of Perovskite solar cells. *Journal of Molecular Structure* 1184: 583-592. https://doi.org/10.1016/j.molstruc.2019.02.042

Becke, A.D. 1993. Density-functional thermochemistry. III. The role of exact exchange. *The Journal of Chemical Physics* 98(7): 5648-5652. https://doi.org/10.1063/1.464913

Benedek, N.A., Snook, I.K., Latham, K. & Yarovsky, I. 2005. Application of numerical basis sets to hydrogen bonded systems: A density functional theory study. *The Journal of Chemical Physics* 122(14): 144102. https://doi.org/10.1063/1.1876152

Bucheli-Witschel, M. & Egli, T. 2001. Environmental fate and microbial degradation of aminopolycarboxylic acids. *FEMS Microbiology Reviews* 25(1): 69-106. https://doi.org/10.1016/s0168-6445(00)00055-3

Casewit, C.J., Colwell, K.S. & Rappe, A.K. 1992a. Application of a universal force field to main group compounds. *Journal of the American Chemical Society* 114(25): 10046-10053. https://doi.org/10.1021/ja00051a042

Casewit, C.J., Colwell, K.S. & Rappe, A.K. 1992b. Application of a universal force field to organic molecules. *Journal of the American Chemical Society* 114(25): 10035-10046. https://doi.org/10.1021/ja00051a041

Delley, B. 2000. From molecules to solids with the DMol^3 approach. *The Journal of Chemical Physics* 113(18): 7756-7764. https://doi.org/10.1063/1.1316015

Delley, B. 1990. An all-electron numerical method for solving the local density functional for polyatomic molecules. *The Journal of Chemical Physics* 92(1): 508-517. https://doi.org/10.1063/1.458452

Ding, X., Li, M., Yang, W., Zhang, K., Zuo, Z., Chen, Y., Yin, X. & Liu, Y. 2020. Experimental and theoretical studies of sodium acetyldithiocarbamate for the removal of Cu^{2+} and Ni^{2+} from aqueous solution. *Journal of Colloid and Interface Science* 579: 330-339. https://doi.org/10.1016/j.jcis.2020.06.074

Dong, W., Wang, R., Li, H., Yang, X., Li, J., Wang, H., Jiang, C. & Wang, Z. 2023. Effects of chelating agents addition on ryegrass extraction of cadmium and lead in artificially contaminated soil. *Water* 15(10): 1929. https://doi.org/10.3390/w15101929

Fredd, C.N. & Fogler, H.S. 1998. The influence of chelating agents on the kinetics of calcite dissolution. *Journal of Colloid and Interface Science* 197(204): 187-197.

Frenier, W.W. 2001. Novel scale removers are developed for dissolving alkaline earth deposits. *Proceedings - SPE International Symposium on Oilfield Chemistry*. pp. 411-423. https://doi.org/10.2523/65027-ms

Frenier, W.W., Rainey, M., Wilson, D., Crump, D. & Jones, L. 2003. A biodegradable chelating agent is developed for stimulation of oil and gas formations. *SPE 80597*. https://doi.org/10.2118/80597-ms

Frenier, W.W., Wilson, D., Crump, D. & Jones, L. 2000. Use of highly acid-soluble chelating agents in well stimulation services. *SPE Reservoir Engineering (Society of Petroleum Engineers)*, No. A. pp. 799-810. https://doi.org/10.2118/63242-ms

Frenkel, D. & Smit, B. 1996. *Understanding Molecular Simulation: From Algorithms to Applications*. Massachusetts: Academic Press, Inc.

Fujieda, H., Maeda, K. & Kato, N. 2018. Efficient and scalable synthesis of glucokinase activator with a chiral thiophenyl-pyrrolidine scaffold. *Organic Process Research & Development* 23(1): 69-77. https://doi.org/10.1021/acs.oprd.8b00354

Guo, L., Ren, X., Zhou, Y., Xu, S., Gong, Y. & Zhang, S. 2017. Theoretical evaluation of the corrosion inhibition performance of 1,3-thiazole and its amino derivatives. *Arabian Journal of Chemistry* 10(1): 121-130. https://doi.org/10.1016/j.arabjc.2015.01.005

Hassan, A., Mahmoud, M. & Patil, S. 2021. Impact of chelating agent salt type on the enhanced oil recovery from carbonate and sandstone reservoirs. *Applied Sciences* 11(15): 7109. https://doi.org/10.3390/app11157109

Hassan, A., Mahmoud, M., Bageri, B.S., Aljawad, M.S., Kamal, M.S., Barri, A.A. & Hussein, I.A. 2020. Applications of chelating agents in the upstream oil and gas industry: A review. *Energy & Fuels* 34(12): 15593-15613. https://doi.org/10.1021/acs.energyfuels.0c03279

Hijazi, M., Krumm, C., Cinar, S., Arns, L., Alachraf, W., Hiller, W., Schrader, W., Winter, R. & Tiller, J.C. 2018. Entropically driven polymeric enzyme inhibitors by end-group directed conjugation. *Chemistry - A European Journal* 24(18): 4523-4527. https://doi.org/https://doi.org/10.1002/chem.201800168

Knepper, T.P. 2003. Synthetic chelating agents and compounds exhibiting complexing properties in the aquatic environment. *Trends in Analytical Chemistry* 22(10): 708-724. https://doi.org/10.1016/S0165-9936(03)01008-2

LePage, J.N., De Wolf, C.A., Bemelaar, J.H. & Nasr-El-Din, H.A. 2011. An environmentally friendly stimulation fluid for high-temperature applications. *SPE Journal* 16(1): 104-110. https://doi.org/10.2118/121709-PA

Mahmoud, M. 2018. Reaction of chelating agents and catalyst with sandstone minerals during matrix acid treatment. *Arabian Journal for Science and Engineering* 43(11): 5745-5756. https://doi.org/10.1007/s13369-017-2962-8

Mahmoud, M.A. & Nasr-El-Din, H.A. 2014. Modeling flow of chelating agents during stimulation of carbonate reservoirs. *Arabian Journal for Science and Engineering* 39(12): 9239-9248. https://doi.org/10.1007/s13369-014-1437-4

Mahmoud, M., Abdelgawad, K., Elkatatny, S., Akram, A. & Stanitzek, T. 2016. Stimulation of seawater injectors by GLDA (Glutamic-Di Acetic Acid). *SPE Drilling & Completion* 31(03): 178-187. https://doi.org/10.2118/172572-pa

Mahmoud, M.A., Nasr-El-Din, H.A., De Wolf, C.A., LePage, J.N. & Bemelaar, J.H. 2011. Evaluation of a new environmentally friendly chelating agent for high-temperature applications. *SPE Journal* 16(3): 559-574. https://doi.org/10.2118/127923-PA

Mandava, S., Ganganna, B., Hwang, J., Jang, Y., Hwang, J., Samala, M., Kim, K-B., Park, H., Lee, J.H., Baek, S.Y. & Lee, J. 2017. Synthesis and structure revision of dimeric tadalafil analogue adulterants in dietary supplements. *Chemical and Pharmaceutical Bulletin* 65(5): 498-503. https://doi.org/10.1248/cpb.c17-00034

Metropolis, N., Rosenbluth, A.W., Rosenbluth, M.N., Teller, A.H. & Teller, E. 1953. Equation of state calculations by fast computing machines. *The Journal of Chemical Physics* 21(6): 1087-1092. https://doi.org/10.1063/1.1699114

Miar, M., Shiroudi, A., Pourshamsian, K., Oliaey, A.R. & Hatamjafari, F. 2021. Theoretical investigations on the HOMO–LUMO gap and global reactivity descriptor studies, natural bond orbital, and nucleus-independent chemical shifts analyses of 3-phenylbenzo[*d*]thiazole-2(3H)-imine and its *para*-substituted derivatives: Solvent and subs. *Journal of Chemical Research* 45(1-2): 147-158. https://doi.org/10.1177/1747519820932091

Muhammad Haziq Ridzwan, Muhammad Haziq, Muhamad Kamil Yaakob, Zubainun Mohamed Zabidi, Ahmad Sazali Hamzah, Zurina Shaameri, Fatin Nur Ain Abdul Rashid, Karimah Kassim, Mohd Fazli Mohammat, Noor Hidayah Pungot, Muhamad Azwan Muhamad Hamali, Ahmad Shalabi Md Sauri, Farhana Jaafar Azuddin, Emily S. Majanun, Yon Azwa Sazali & M. Zuhaili Kashim. 2022. Computational insight into the quantum chemistry, interaction and adsorption energy of aminopolycarboxylic acid chelating agents towards metal cations. *Computational and Theoretical Chemistry* 1208: 113579. https://doi.org/10.1016/j.comptc.2021.113579

Noureddine, O., Issaoui, N., Gatfaoui, S., Al-dossary, O. & Marouani, H. 2021. Quantum chemical calculations, spectroscopic properties and molecular docking studies of a novel piperazine derivative. *Journal of King Saud University - Science* 33(2): 101283. https://doi.org/10.1016/j.jksus.2020.101283

Obot, I.B., Kaya, S., Kaya, C. & Tüzün, B. 2016. Density functional theory (DFT) modeling and Monte Carlo simulation assessment of inhibition performance of some carbohydrazide Schiff bases for steel corrosion. *Physica E: Low-Dimensional Systems and Nanostructures* 80: 82-90. https://doi.org/10.1016/j.physe.2016.01.024

Pilli, S.R., Banerjee, T. & Mohanty, K. 2015. HOMO - LUMO energy interactions between endocrine disrupting chemicals and ionic liquids using the density functional theory: Evaluation and comparison. *Journal of Molecular Liquids* 207: 112-124. https://doi.org/10.1016/j.molliq.2015.03.019

Rappe, A.K., Colwell, K.S. & Casewit, C.J. 1993. Application of a universal force field to metal complexes. *Inorganic Chemistry* 32(16): 3438-3450. https://doi.org/10.1021/ic00068a012

Rappe, A.K., Casewit, C.J., Colwell, K.S., Goddard III, W.A. & Skiff, W.M. 1992. UFF, a full periodic table force field for molecular mechanics and molecular dynamics simulations. *Journal of the American Chemical Society* 114(25): 10024-10035. https://doi.org/10.1021/ja00051a040

Repo, E., Warchoł, J.K., Bhatnagar, A., Mudhoo, A. & Sillanpää, M. 2013. Aminopolycarboxylic acid functionalized adsorbents for heavy metals removal from water. *Water Research* 47(14): 4812-4832. https://doi.org/10.1016/j.watres.2013.06.020

Singh, A., Ansari, K.R., Quraishi, M.A. & Lin, Y. 2019. Investigation of corrosion inhibitors adsorption on metals using density functional theory and molecular dynamics simulation. *Corrosion Inhibitors*, edited by Singh, A. IntechOpen. https://doi.org/10.5772/intechopen.84126

Stephens, P.J., Devlin, F.J., Chabalowski, C.F. & Frisch, M.J. 1994. *Ab initio* calculation of vibrational absorption and circular dichroism spectra using density functional force fields. *The Journal of Physical Chemistry* 98(45): 11623-11627. https://doi.org/10.1021/j100096a001

Tuerk, H., Weber, H., Kischkel, D. & Franke, J. 2019. *Formulations and Production and Use Thereof.* Patent No. US 10,844,326 B2.

Xu, Y., Zhang, S., Li, W., Guo, L., Xu, S., Feng, L. & Madkour, L.H. 2018. Experimental and theoretical investigations of some pyrazolo-pyrimidine derivatives as corrosion inhibitors on copper in sulfuric acid solution. *Applied Surface Science* 459: 612-620. https://doi.org/10.1016/j.apsusc.2018.08.037

Yusuf, T.L., Oladipo, S.D., Zamisa, S., Kumalo, H.M., Lawal, I.A., Lawal, M.M. & Mabuba, N. 2021. Design of new Schiff-base copper(II) complexes: Synthesis, crystal structures, DFT study, and binding potency toward cytochrome P450 3A4. *ACS Omega* 6(21): 13704-13718. https://doi.org/10.1021/acsomega.1c00906

Ziemlak, L.W., Bullock, J.L., Bersworth, F.C. & Martell, A.E. 1950. Carboxymethylation of amines. III. Preparation of substituted glycines. *The Journal of Organic Chemistry* 15(2): 255-258. https://doi.org/10.1021/jo01148a007

*Corresponding author; email: mohdfazli@uitm.edu.my